MESOMETEOROLOGY PROJECT

Department of the Geophysical Sciences
The University of Chicago

DETERMINATION OF MASS OUTFLOW FROM A THUNDERSTORM COMPLEX USING ATS III PICTURES

by

T. T. Fujita and D. L. Bradbury
The University of Chicago

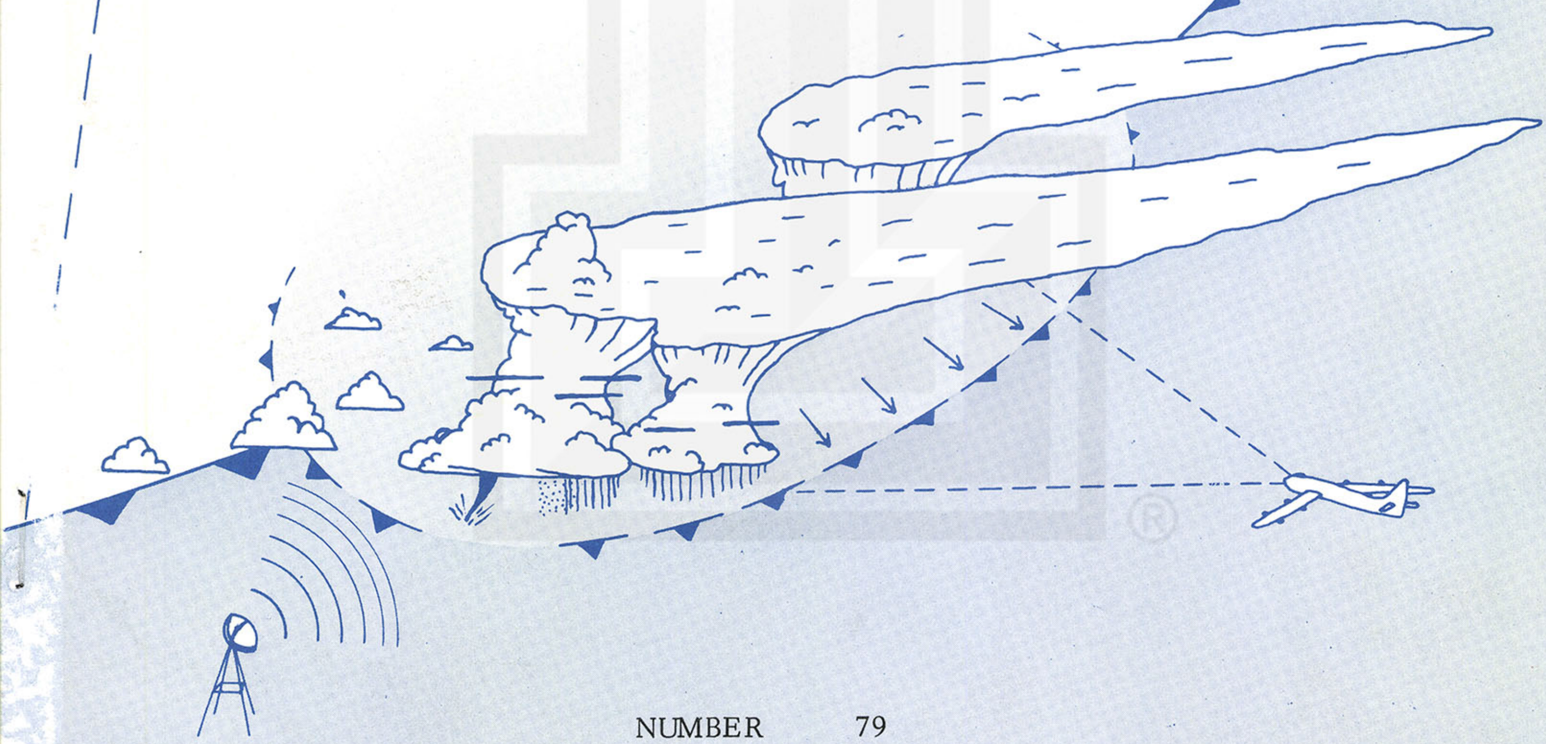

NUMBER 79
April 1969

MESOMETEOROLOGY PROJECT --- RESEARCH PAPERS

1.* Report on the Chicago Tornado of March 4, 1961 - Rodger A. Brown and Tetsuya Fujita

2.* Index to the NSSP Surface Network - Tetsuya Fujita

3.* Outline of a Technique for Precise Rectification of Satellite Cloud Photographs - Tetsuya Fujita

4.* Horizontal Structure of Mountain Winds - Henry A. Brown

5.* An Investigation of Developmental Processes of the Wake Depression Through Excess Pressure Analysis of Nocturnal Showers - Joseph L. Goldman

6.* Precipitation in the 1960 Flagstaff Mesometeorological Network - Kenneth A. Styber

7.** On a Method of Single- and Dual-Image Photogrammetry of Panoramic Aerial Photographs - Tetsuya Fujita

8. A Review of Researches on Analytical Mesometeorology - Tetsuya Fujita

9.* Meteorological Interpretations of Convective Nephsystems Appearing in TIROS Cloud Photographs - Tetsuya Fujita, Toshimitsu Ushijima, William A. Hass, and George T. Dellert, Jr.

10.* Study of the Development of Prefrontal Squall-Systems Using NSSP Network Data - Joseph L. Goldman

11. Analysis of Selected Aircraft Data from NSSP Operation, 1962 - Tetsuya Fujita

12. Study of a Long Condensation Trail Photographed by TIROS I - Toshimitsu Ushijima

13. A Technique for Precise Analysis of Satellite Data; Volume I - Photogrammetry (Published as MSL Report No. 14) - Tetsuya Fujita

14. Investigation of a Summer Jet Stream Using TIROS and Aerological Data - Kozo Ninomiya

15. Outline of a Theory and Examples for Precise Analysis of Satellite Radiation Data - Tetsuya Fujita

16. Preliminary Result of Analysis of the Cumulonimbus Cloud of April 21, 1961 - Tetsuya Fujita and James Arnold

17. A Technique for Precise Analysis of Satellite Photographs - Tetsuya Fujita

18.* Evaluation of Limb Darkening from TIROS III Radiation Data - S.H.H. Larsen, Tetsuya Fujita, and W.L. Fletcher

19. Synoptic Interpretation of TIROS III Measurements of Infrared Radiation - Finn Pedersen and Tetsuya Fujita

20.* TIROS III Measurements of Terrestrial Radiation and Reflected and Scattered Solar Radiation - S.H.H. Larsen, Tetsuya Fujita, and W.L. Fletcher

21. On the Low-level Structure of a Squall Line - Henry A. Brown

22.* Thunderstorms and the Low-level Jet - William D. Bonner

23.* The Mesoanalysis of an Organized Convective System - Henry A. Brown

24. Preliminary Radar and Photogrammetric Study of the Illinois Tornadoes of April 17 and 22, 1963 - Joseph L. Goldman and Tetsuya Fujita

25. Use of TIROS Pictures for Studies of the Internal Structure of Tropical Storms - Tetsuya Fujita with Rectified Pictures from TIROS I Orbit 125, R/O 128 - Toshimitsu Ushijima

26. An Experiment in the Determination of Geostrophic and Isallobaric Winds from NSSP Pressure Data - William Bonner

27. Proposed Mechanism of Hook Echo Formation - Tetsuya Fujita with a Preliminary Mesosynoptic Analysis of Tornado Cyclone Case of May 26, 1963 - Tetsuya Fujita and Robbi Stuhmer

28. The Decaying Stage of Hurricane Anna of July 1961 as Portrayed by TIROS Cloud Photographs and Infrared Radiation from the Top of the Storm - Tetsuya Fujita and James Arnold

29. A Technique for Precise Analysis of Satellite Data, Volume II - Radiation Analysis, Section 6. Fixed-Position Scanning - Tetsuya Fujita

30. Evaluation of Errors in the Graphical Rectification of Satellite Photographs - Tetsuya Fujita

31. Tables of Scan Nadir and Horizontal Angles - William D. Bonner

32. A Simplified Grid Technique for Determining Scan Lines Generated by the TIROS Scanning Radiometer - James E. Arnold

33. A Study of Cumulus Clouds over the Flagstaff Research Network with the Use of U-2 Photographs - Dorothy L. Bradbury and Tetsuya Fujita

34. The Scanning Printer and Its Application to Detailed Analysis of Satellite Radiation Data - Tetsuya Fujita

35. Synoptic Study of Cold Air Outbreak over the Mediterranean using Satellite Photographs and Radiation Data - Aasmund Rabbe and Tetsuya Fujita

36. Accurate Calibration of Doppler Winds for their use in the Computation of Mesoscale Wind Fields - Tetsuya Fujita

37. Proposed Operation of Intrumented Aircraft for Research on Moisture Fronts and Wake Depressions - Tetsuya Fujita and Dorothy L. Bradbury

38. Statistical and Kinematical Properties of the Low-level Jet Stream - William D. Bonner

39. The Illinois Tornadoes of 17 and 22 April 1963 - Joseph L. Goldman

40. Resolution of the Nimbus High Resolution Infrared Radiometer - Tetsuya Fujita and William R. Bandeen

41. On the Determination of the Exchange Coefficients in Convective Clouds - Rodger A. Brown

* Out of Print
** To be published

(Continued on back cover)

SATELLITE AND MESOMETEOROLOGY RESEARCH PROJECT
Department of the Geophysical Sciences
The University of Chicago

DETERMINATION OF MASS OUTFLOW FROM A THUNDERSTORM COMPLEX USING ATS III PICTURES*

by

T. T. Fujita and D. L. Bradbury
The University of Chicago

SMRP Research Paper No. 79
April 1969

*The research reported in this paper has been supported by the National Aeronautics and Space Administration under grant NGR 14-001-008 and the Environmental Science Service Administration under grants USESSA E-22-45-68-(G) and ESSA E-198-68-(G).

DETERMINATION OF MASS OUTFLOW FROM A THUNDERSTORM COMPLEX USING ATS III PICTURES*

by

T. T. Fujita and D. L. Bradbury

The University of Chicago

ABSTRACT

Presented in this paper are some preliminary results of the Tornado Watch Experiment, 1968. Two excellent cases of tornado outbreaks over the Midwest were photographed at 14-min intervals by ATS III. One of the cases occurred on April 19 and was studied together with aerological and surface data, radar pictures, and cloud displacement computation from ATS pictures. It was found that there was little evidence of mesoscale divergence of high-cloud velocities prior to the storm formation. As the storm grew rapidly, a significant divergence at the anvil level modified the field of jetstream-cloud velocities. This preliminary study resulted in a number of new questions to be answered in the future rather than solving previously unanswered questions. It is expected that the 1969 experiment to be conducted again by NASA and ESSA will include acquisition of radar and synoptic data so that our effort can be expanded toward the solution of complicated phenomena of severe-storm formation over the Midwest.

1. Introduction

After the first meteorological satellite, TIROS I, was launched on 1 April 1960, various comments and ideas as to the use of satellite data in severe storm research over the midwestern United States have arisen in our scientific communities. Satellite data are, of course, of extreme value in depicting cloud characteristics over vast oceanic areas where few synoptic reports are available. The Midwest region of the United States, a major severe-storm bearing area in the spring, is covered by a network of reporting stations about 100-mi apart and of weather radars which scan every square mile, if not every square inch, of the storm-producing area. The present state of the art of prediction involving physical and dynamical processes of severe storm formation and subsequent development still requires more basic research by

*The research reported in this paper has been supported by the National Aeronautics and Space Administration under grant NGR 14-001-008 and the Environmental Science Services Administration under grants USESSA E-22-45-68-(G) and ESSA E-198-68-(G).

using a more-advanced network of stations, radar, and satellite technology.

Cumulus convection taking place in random or line configuration as that studied by Kuettner (1959) rarely develops into a severe thunderstorm as long as the convective elements maintain their uniform density over a more or less uniformly heated area. One of the best examples of such a cloud-street convection over the southern Midwest appears in a mosaic satellite picture (Fig. 1) taken by a Russian satellite, COSMOS 144, on 31 March 1967. COSMOS 144 was launched on 28 February 1967 in an 81.2 deg-inclination orbit with a mean height of 592 km and a 96.92-min period. The nominal resolution of one to two kilometers permits us to see a large number of small cumuli within each cloud street. This COSMOS picture presents a remarkable example of amalgamation of several cloud streets into large cloud bands consisting of large cloud cells over 30 km in diameter. Note that cumulus elements near the Gulf Coast are of 2- to 3-mile diameter. As the moist air travels inland the growth of these elements is shown quite clearly. Rain showers or thunderstorms were reported in the area of large cloud cells. Schuetz and Fritz (1961) also noted that the spacing of cloud streets over heated land was less than over the ocean due to the increase in size of the cloud elements.

At 1935Z, some 75-min after the COSMOS picture was taken, ESSA III, in a 79.) deg-inclination orbit with a mean height of 1650 km and a 114.5-min period, took the cloud picture shown in Fig. 2. Due to its altitude, about 2.8 times the COSMOS altitude, the ESSA III AVCS picture does not reveal cumulus streets but a number of large storm streets is apparent. From these pictures, together with radar pictures over the area, it is feasible to study the mode of cloud-street to cloud-band convection which will give rise to cumulus and to mild-storm convection.

When the scope of storm studies extends into dynamical and physical aspects of severe-storm producing nephsystems, it becomes necessary to learn more about the time changes in storm systems. A geosynchronous satellite offers an ideal platform for such a time-change study. In this respect, ATS pictures do add a new dimension in relation to both growth rate and the rate of displacement.

The purpose of this paper is to obtain the cloud-velocity fields related to the development of large thunderstorms over the Midwest.

2. Severe Storms Situation of 19 April 1968

During the Tornado Watch Experiment in the spring of 1968 predictions of outbreaks of tornadoes were made in order to alert NASA to take a whole-day sequence of half-scan pictures at about 14-min intervals by using ATS III, then located at 85W above the equator.

The conventional surface analyses shown in Fig. 3 indicate that radar echoes (solid black areas) are located over the region where the advected moist air meets the front of dry air from the west. The structure of the dry front is quite similar to that studied by Beebe (1958), Fujita (1958), and others. A jetstream of over 100 km from the southwest prevailed over the region where the two black arrows in the figure would intersect when extended. The area of echo development, therefore, took place where the high-level jet overran the axis of low-level moisture inflow, which often coincides with that of a low-level jet. Such a climatological evidence was studied notably by Fawbush, et al. (1951), Means (1952) and Fawbush and Miller (1953).

Superimposed upon the surface chart with radar echoes are the areas of large convective clouds appearing in the ATS III picture nearest to 0000Z, 20 April 1968. As can be seen, the majority of echoes in the central convective band extending along the 97W meridian were located near the southwestern portion of the cloud areas photographed by ATS III, suggesting that anvil materials had been drawn downwind.

Although the development of these storms is confined to the region of expected release of instability, it is almost impossible to find the reasons for the development of individial storms. A detailed examination of surface winds does not show the existence of a convergence field in the scale of each convective nephsystem. The distribution of upper-air stations, shown in the figure by three-letter designators such as AMA, OKC, etc., is not dense enough to find the field of motion related to each nephsystem.

3. Interpretation of High-Cloud Velocity

Using the cloud-velocity computation technique described by Fujita, et. al. (1968), a large number of clouds with faint edges, which may be called fuzzy clouds, were tracked on consecutive ATS cloud picture frames to compute their velocity. Most of these clouds moved at very high speeds, up to 115 kt, slightly slower than the maximum jet-speed measured in the vicinity.

In order to determine the representative pressure corresponding to the measured fuzzy-cloud velocities, a hodograph of wind velocities at 100-mb intervals was constructed for all upper-air stations in the area of analysis. Four of these examples are shown in Fig. 4. As shown in the case of the Fort Worth sounding black circles were plotted and connected to form a hodograph. Then the velocity of the fuzzy cloud nearest to the station was added with 10 and 15 percent error circles drawn around the end point of the velocity vector.

Statistics revealed that over 85 percent of the 200-mb wind was found inside each 10 percent error circle, suggesting that ATS-measured cloud velocities represent the 250-mb velocity within a 10 percent error. The examples from Abilene, Victoria, and Del Rio equally reveal that it would be reasonably accurate to use fuzzy-cloud velocities as being representative of 250-mb wind velocities.

About 20 to 50 fuzzy clouds within a 5-deg box inside a jetstream can be tracked for such velocity computations. An attempt was made, therefore, to detect detailed variations in the flow patterns of jetstream cirrus related to the development of severe thunderstorms.

4. High-Level Flow Prior to the Storm Development

The diamond-shaped cloud shown in Fig. 3 to the southeast of GSW extending 150 x 250 km in horizontal dimensions is of extreme interest. This type of an extensive cloud appearing in the shape of a square was first photographed on 15 May 1960 by TIROS I. After Whitney and Fritz (1961) studied that square cloud in detail meteorologists have been wondering as to the conditions leading to the development of such a cloud.

Shown in Fig. 5A is a section of an ATS picture taken in a 14-min interval sequence. The scan time increasing from north to south was 2133Z at the picture center. At this time, a couple of small echoes was observed at the range of about 200 n mi northwest of the Galveston, Texas radar. The first detectable echo at 2112Z was located near the point almost equidistant from ABI, GSW, and VCT, where two clouds which are slightly whiter than the environment are visible in the photograph. Fuzzy clouds extending from southwest to northeast are the jetstream cirrus travelling at a high rate of displacement.

The boundaries of clouds shown in Fig. 5A were sketched in Fig. 5B with the convective clouds indicated with stippled areas and radar echoes in solid black. Plotted in this figure are the velocity vectors of the fuzzy clouds identified by small black circles and those of suspected middle-type clouds indicated by small open circles. Numbers entered by each velocity vector denote the cloud speed in kt computed from four consecutive pictures taken during a 55-min period following 2106Z, 19 April 1968.

It is seen that the directions of fuzzy cloud displacement, which, according to the previous section, are supposed to represent the 250-mb flow, are parallel to each other over the region of the echo growth. The first indication of the diamond-shaped cloud is also shown in this figure. Cloud speed across the jetstream increases from about 60 kt to 100 kt toward the northwest. The maximum jet-speeds are found near the northwestern edge of the jetstream cirrus. This feature coincides with the cloud and jetspeed relationship found by Oliver, Anderson, and Ferguson (1964) and Whiney, Timchalk and Gray (1966) using non-ATS satellite pictures.

An effort was made to compute patterns of the mesoscale divergence field as related to the development or generating stage of the diamond-shaped cloud. It was expected that an upper divergence field would be obtained but instead the results showed a non-divergent but highly anticyclonic field of motion. Generally speaking, the area of interest is located inside the forward right sector of a jetstream or the right sector of the exit region according to Newton's (1954) study of jetstreams. Ageostrophic flow due to the deceleration of high speed flow overtaking the jet-core region will result in a synoptic-scale convergence field at the jetstream level. Such dynamical characteristics were reviewed by Reiter (1963).

Analyses of high-cloud displacement prior to or just after the initial echoes of this diamond-shaped cloud revealed significant features in the vorticity and divergence field**

** Fujita has developed a method of filming ATS pictures on Lagrangian coordinates by moving a camera with a specific cloud. A test movie entitled, "Fishbone-like Jetstream Cirrus" shows convincingly the relative motion field which has never before been recognized in Eulerian-coordinate ATS movies. Future studies using this method might reveal dynamical aspects of flows at jetstream levels related to storm development.

which could be tied into the cause of the cloud formation.

5. Motion of High Clouds After the Storm Development

Less than two hours after the picture of Fig. 5A was taken the cloud grew into a large diamond-shaped nephsystem, shown in Fig. 6A. It should be noted that a clearing of jetstream cirrus took place practically all around the nephsystem, suggesting the existence of the descending motion which dissipated the cirrus.

Although a two-hour period seems to be rather short for such a dramatic growth, Byers' and Braham's (1949) report, The Thunderstorm, revealed a very short cycle of individual cells each of which does contribute to the overall growth of such a diamond-shaped cloud. Fujita (1963) presented an analysis of the TIROS square cloud of 15 May 1960 mentioned in the previous section showing that the cloud boundary estimated from the passage of the shadow line over the NSSL network expanded explosively in about 2. 5 hours into a 200 x 400 km diamond-shaped cloud. Such a growth rate of an amalgamated storm system will not be uncommon.

The field of high-cloud velocities in Fig. 6B shows a dramatic change as compared with those two hours earlier. Although high-cloud speeds near the jetstream axis running along the northwestern edge remained practically unchanged, the flow around the diamond-shaped cloud changed into a remarkable mesoscale difluence pattern. The figure reveals that the upwind jetstream flow with about 8--kt speed diverged by almost 45 degrees.

Such a mesoscale modification of flow at the jetstream level due to an explosive development of a large convective system seems to be quite natural because anvil materials are transported from lower levels where moist air converging into the storm originated. Radar echoes inside the diamond-shaped cloud were moving at about 45 kt which is, of course, much slower than those of the high cloud which existed in the cloud area prior to the cloud formation. Motion of radar echoes and clouds under the influence of vertical wind shear was studied by Newton (1963), Newton and Fankhauser (1964), Fujita and Grandoso (1968), and many others. All their results show that echo speeds are slower than the cirrus-level flow speed.

6. Velocity of High Clouds Relative to Radar Echoes

Because of the fact that both radar echoes and high clouds are moving at different rates, it would be helpful in understanding their interaction if we would construct a relative flow chart by simply subtracting the mean echo velocity from each of the measured high-cloud velocities. Figure 7 represents the relative motion field thus constructed. A mean echo velocity of 45 kt from 240 degs was used in computing relative velocity vectors. It is obvious that a group of large convective nephsystems will act as an obstacle to large-scale jetstream flow. By presenting the flow pattern in a relative coordinate system, however, we are able to show more effectively the influences of convective systems upon the high-level flow.

The question may arise as to the net effect of convective systems upon the over-running jetstream. Do these systems weaken the flow at high levels? If the answer to this question is in the affirmative, we would expect that a jetstream flow will weaken if too many convective clouds penetrate through the level of jetstream cirrus.

Computation of the two-dimensional mass flux inside the relative flow in Fig. 8 suggests, however, the answer should be first "yes" and then "no" later. The mass flux was computed along each of the lines A, B, C, . . . M which are orthogonal trajectories to smoothed relative stream lines. Results indicated that the upwind mass flux measured along A was 83×10^5 $m^2 sec^{-1}$, but it decreased to 81 or 82 before reaching the convective area due probably to the obstacle effect. Upon reaching the convective area, however, the mass flux started increasing sharply because convective storms transport low-level mass upward into the upper troposphere.

The significant increase which took place in convective areas implies that the amount of the descending air all around convective cloud boundaries is much less than that of the rising air through the active regions inside the cloud. An increase in the horizontal mass flux from 83 to $112 \times 10^5 m^2 sec^{-2}$ between up- and downwind sides of the storm area gives a 35 percent increase in the horizontal mass flux at about 250 mb height. The question still remains if such an increase is the result of convective activity which a jetstream does not care about or whether a jetstream initially supplies a slight upper divergence field expecting that subsequent development of convective storms would consequently increase the horizontal mass flux.

7. Conclusions

The first year of the Tornado Watch Experiment using ATS III turned out to be very useful in questioning physical and dynamical processes pertaining to the origin and the development of large convective storms. It was found that by using four pictures taken at about 14-min intervals and analyzed together gives velocity of high cloud with an accuracy much better than 10 percent error. If picture intervals exceed 20 min the continuity of fast moving and quickly changing cloud elements could be lost, thus inhibiting proper tracking of individual elements.

Through computations of cloud displacements, it is feasible to construct synoptic charts of high-cloud velocities almost continuously during the sunlit hours if a proper picture sequence is available. In order to interpret these cloud velocities meteorologically, it is necessary to obtain simultaneous radar pictures and surface and upper-air observations. A combined analysis of these data is the key to the understanding of severe-storm producing thunderstorms over the Midwest.

REFERENCES

Beebe, R. G., 1958: An instability line development as observed by the tornado research plane. J. Meteor., 15, 278-282.

Byers, H. R., and R. R. Braham, 1949: The Thunderstorm. Washington, D. C., Government Printing Office, 287 pp.

Fawbush, E. J., R. C. Miller, and L. G. Starrett, 1951: An empirical method of forecasting tornado development. Bull. Amer. Meteor. Soc., 32, 1-9.

_____, and R. C. Miller, 1953: The tornado situation of 17 March 1951. Bull. Amer. Meteor. Soc., 34, 139-145.

Fujita, T., 1958: Structure and movement of a dry front. Bull. Amer. Meteor. Soc., 39, 574-582.

_____, 1963: Analytical mesometeorology: a review. Meteor. Monogr., 5, No. 27, 77-125.

_____, D. L. Bradbury, C. Murino, and L. Hull, 1968: A study of mesoscale cloud motions computed from ATS-I and terrestrial photographs. SMRP Research Paper No. 71, University of Chicago, 25 pp.

_____, and H. Grandoso, 1968: Split of a thunderstorm into anticyclonic and cyclonic storms and their motion as determined from numerical model experiments. J. Atmos. Sci., 25, 416-439.

Kuettner, J., 1959: The band structure of the atmosphere. Tellus, 11, 267-294.

Means, L. L., 1952: On thunderstorm forecasting in the Central United States. Mon. Wea. Rev., 80, 165-189.

Newton, C. W., 1954: Frontogenesis and frontolysis as a three-dimensional process. J. Meteor., 11, 449-461.

_____, 1963: Dynamics of severe convective storms. Meteor. Monogr., 5, No. 27, 33-58.

_____, and J. C. Fankhauser, 1964: On the movement of convective storms, with emphasis on size discrimination in relation to water-budget requirements. J. Appl. Meteor., 3, 651-668.

Oliver, V. J., R. K. Anderson, and E. W. Ferguson, 1964: Some examples of the detection of jet streams from TIROS photographs. Mon. Wea. Rev., 92, 441-448.

Reiter, E. R., 1963: Jet-stream meteorology. Chicago, Illinois, University of Chicago Press, 515 pp.

Schuetz, J. and S. Fritz, 1961: Cloud streets over the Caribbean Sea. Mon. Wea. Rev., 89, 375-382.

Whitney, L. F., Jr., and S. Fritz, 1961: A tornado-producing cloud pattern seen from TIROS I. Bull. Amer. Meteor. Soc., 42, 603-614.

_____, A. Timchalk, and T. I. Gray, Jr., 1966: On locating jet streams from TIROS photographs. Mon. Wea. Rev., 94, 231-236.

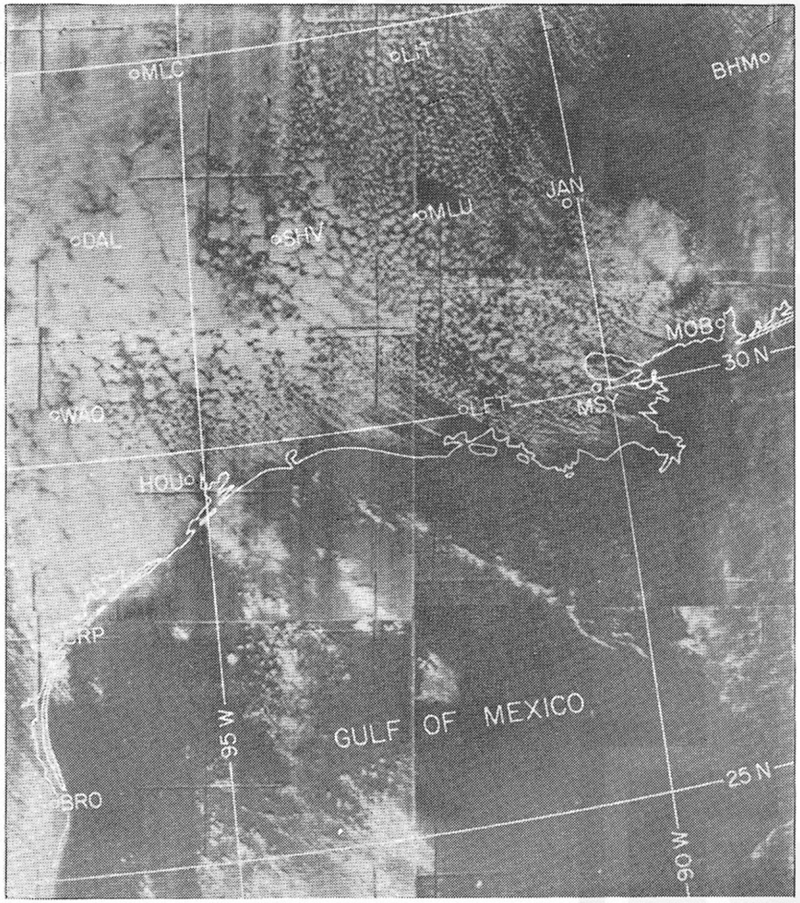

Fig. 1. COSMOS-144 view from 590-km altitude. 1820Z, 31 March 1967.

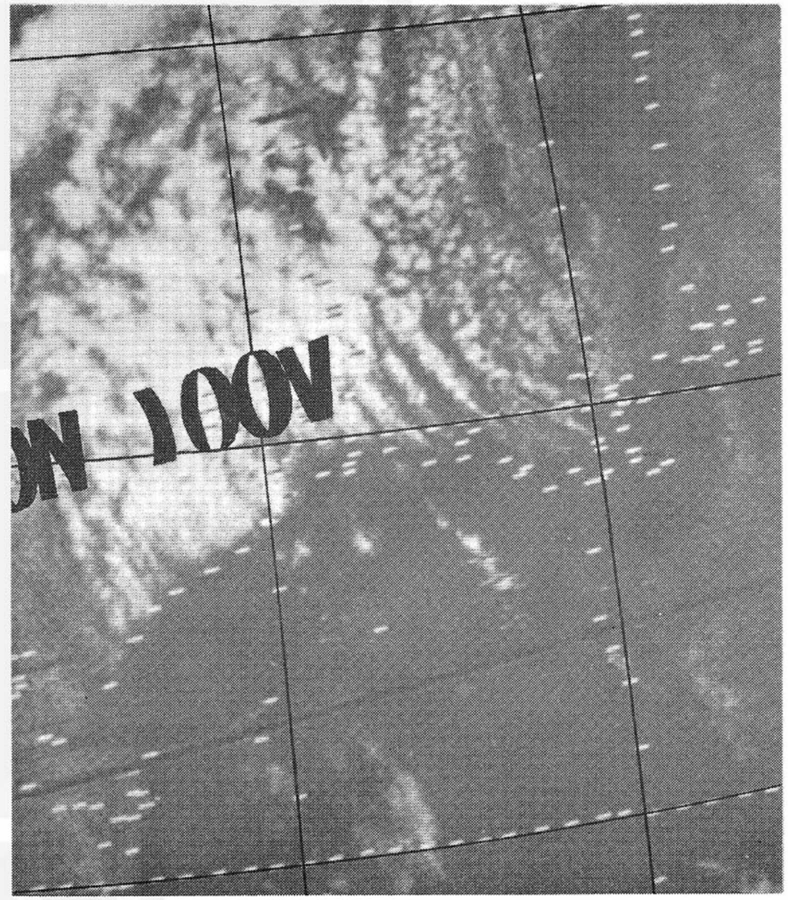

Fig. 2. ESSA-3 view from 1650-km altitude, 1935Z, 31 March 1967.

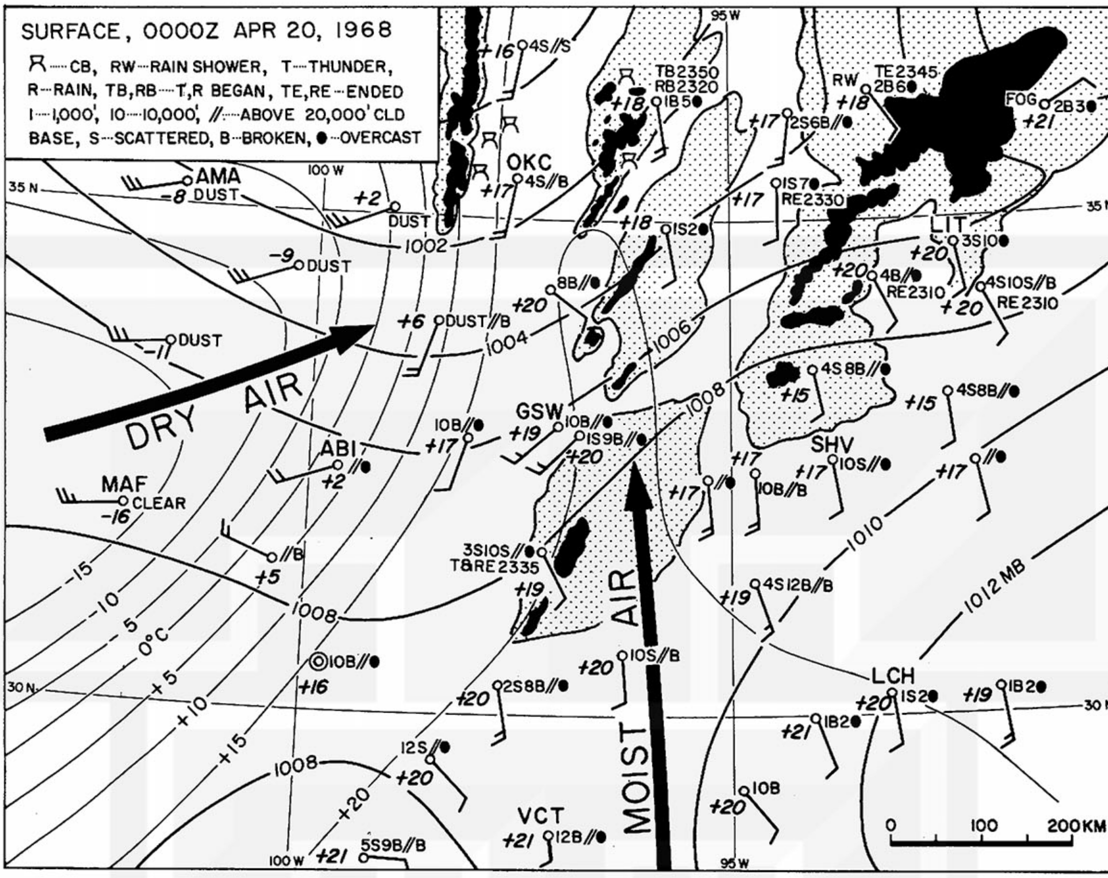

Fig. 3. Surface chart with radar echoes and areas of convective clouds. 0000Z, 20 April 1968.

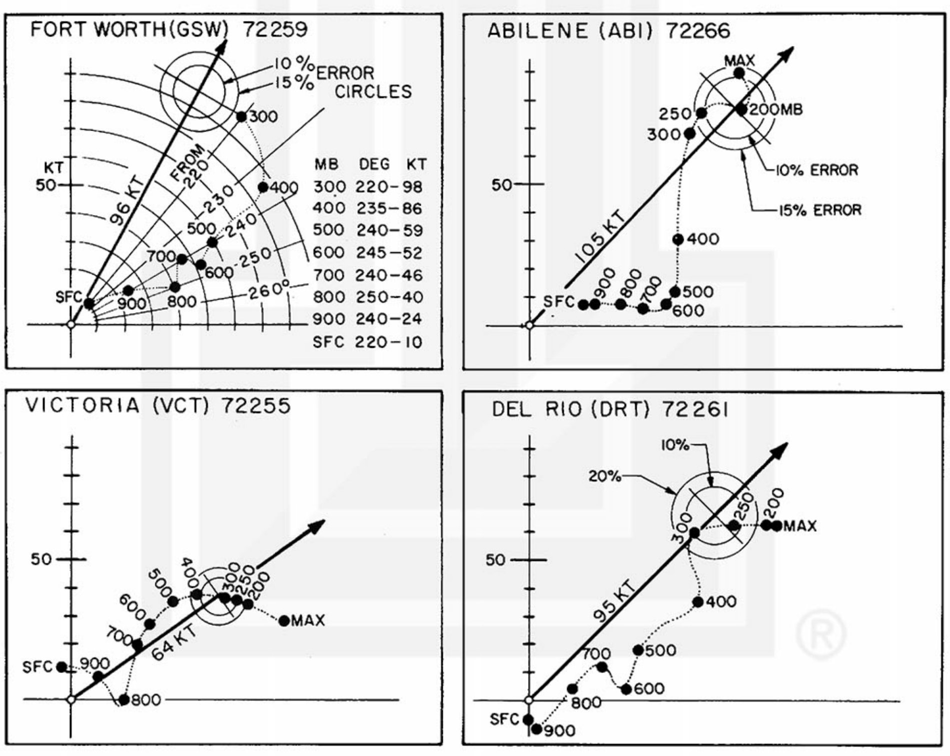

Fig. 4. High-cloud velocities plotted in wind-velocity hodographs.

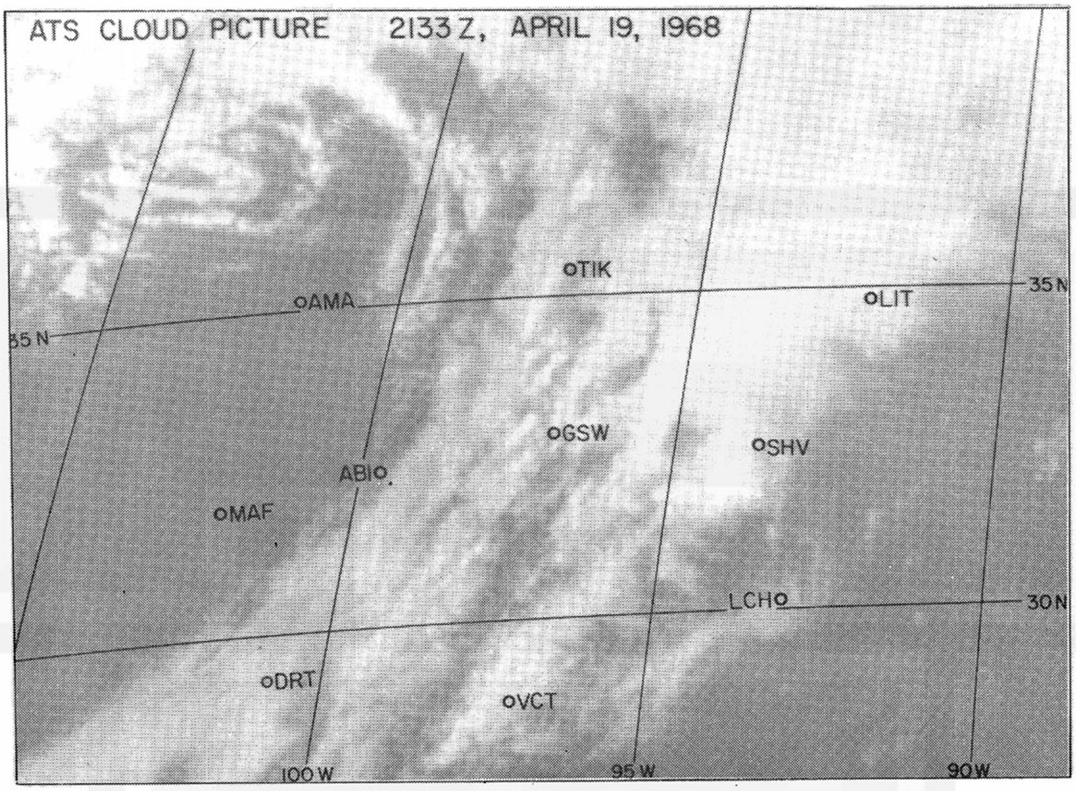

Fig. 5A. A digitized ATS III picture at 2133Z, 19 April 1968.

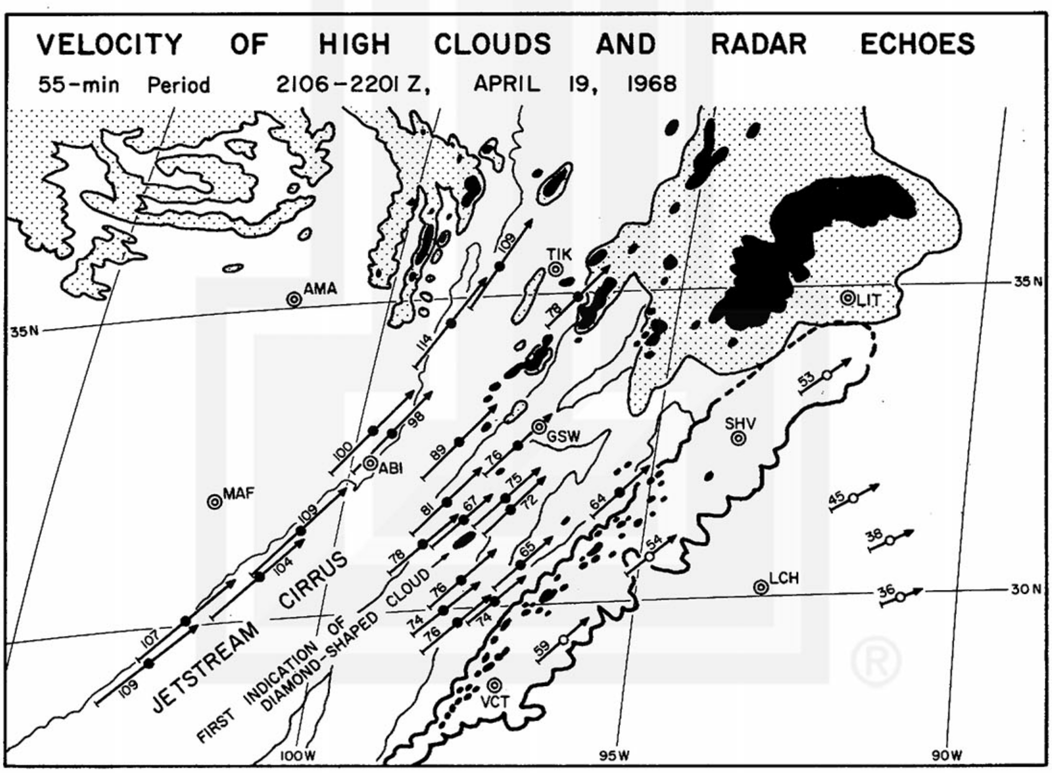

Fig. 5B. Field of high-cloud velocity prior to the development of a diamond-shaped cloud.

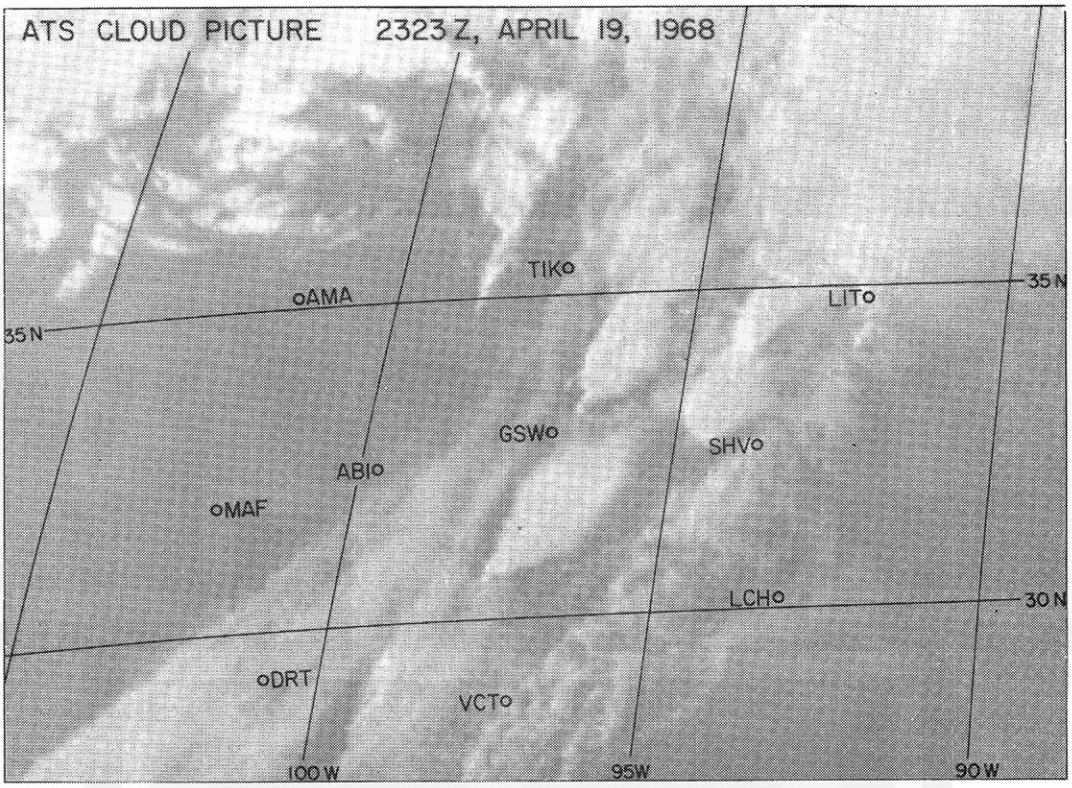

Fig. 6A. A digitized ATS III picture at 2323Z, 19 April 1968.

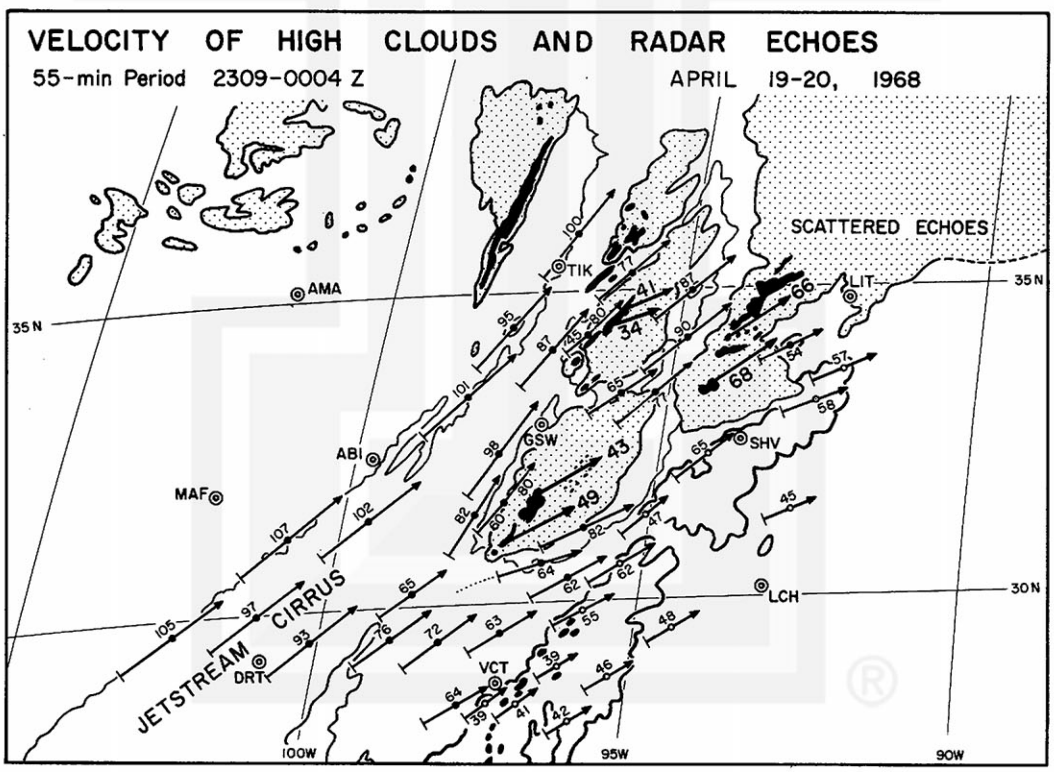

Fig. 6B. Abrupt change in the velocity field of high clouds some two hours after the time of Fig. 5B.

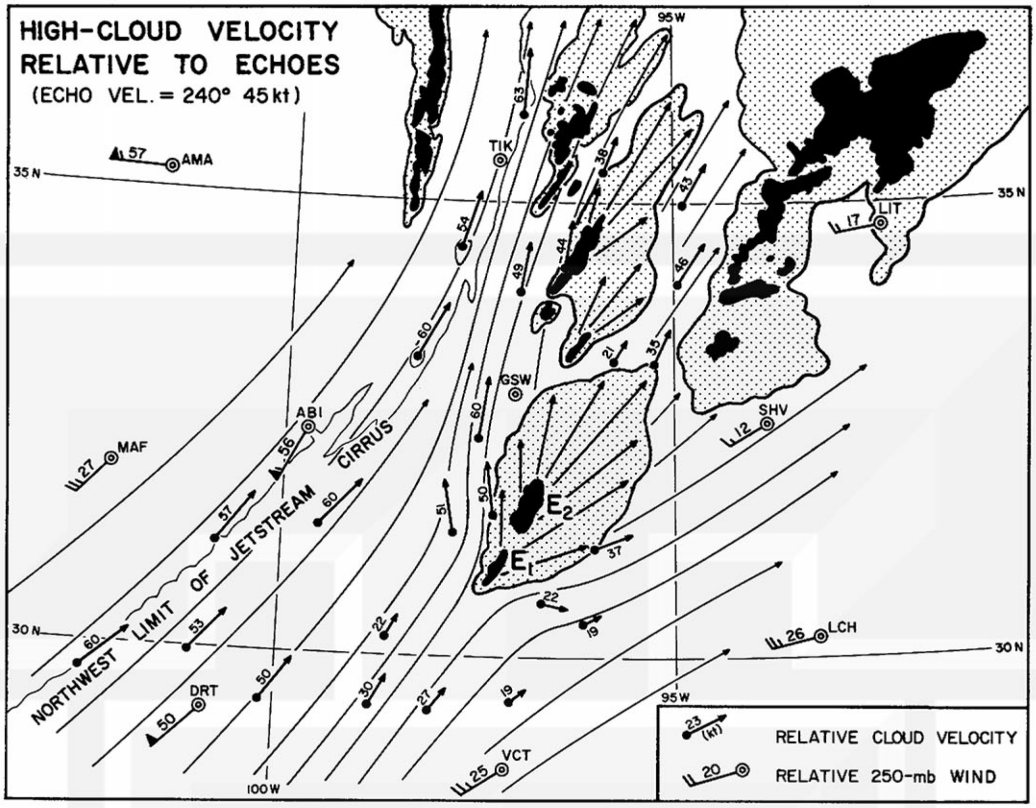

Fig. 7. High-cloud velocity relative to radar echoes inside the diamond-shaped cloud.

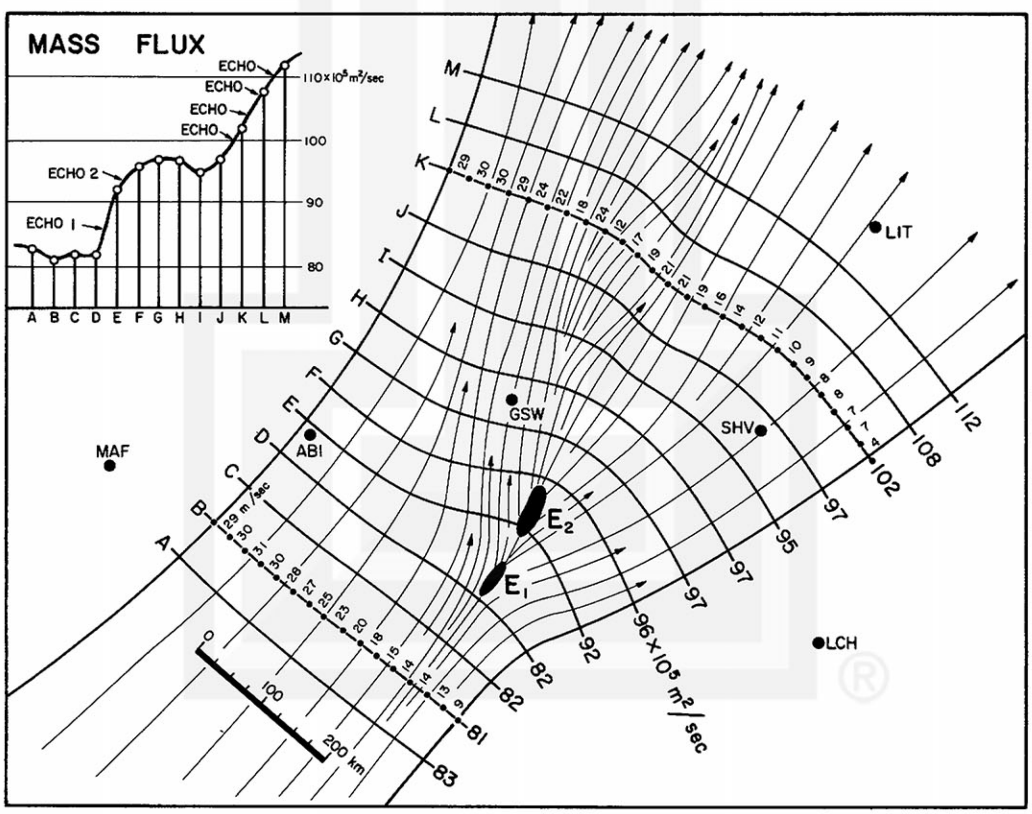

Fig. 8. Horizontal mass flux at about 250 mb computed from cloud displacements.

MESOMETEOROLOGY PROJECT - - - RESEARCH PAPERS

(Continued from front cover)

42.* A Study of Factors Contributing to Dissipation of Energy in a Developing Cumulonimbus - Rodger A. Brown and Tetsuya Fujita

43. A Program for Computer Gridding of Satellite Photographs for Mesoscale Research - William D. Bonner

44. Comparison of Grassland Surface Temperatures Measured by TIROS VII and Airborne Radiometers under Clear Sky and Cirriform Cloud Conditions - Ronald M. Reap

45. Death Valley Temperature Analysis Utilizing Nimbus I Infrared Data and Ground-Based Measurements - Ronald M. Reap and Tetsuya Fujita

46. On the "Thunderstorm-High Controversy" - Rodger A. Brown

47. Application of Precise Fujita Method on Nimbus I Photo Gridding - Lt. Cmd. Ruben Nasta

48. A Proposed Method of Estimating Cloud-top Temperature, Cloud Cover, and Emissivity and Whiteness of Clouds from Short- and Long-wave Radiation Data Obtained by TIROS Scanning Radiometers - T. Fujita and H. Grandoso

49. Aerial Survey of the Palm Sunday Tornadoes of April 11, 1965 - Tetsuya Fujita

50. Early Stage of Tornado Development as Revealed by Satellite Photographs - Tetsuya Fujita

51. Features and Motions of Radar Echoes on Palm Sunday, 1965 - D. L. Bradbury and T. Fujita

52. Stability and Differential Advection Associated with Tornado Development - Tetsuya Fujita and Dorothy L. Bradbury

53. Estimated Wind Speeds of the Palm Sunday Tornadoes - Tetsuya Fujita

54. On the Determination of Exchange Coefficients: Part II - Rotating and Nonrotating Convective Currents - Rodger A. Brown

55. Satellite Meteorological Study of Evaporation and Cloud Formation over the Western Pacific under the Influence of the Winter Monsoon - K. Tsuchiya and T. Fujita

56. A Proposed Mechanism of Snowstorm Mesojet over Japan under the Influence of the Winter Monsoon - T. Fujita and K. Tsuchiya

57. Some Effects of Lake Michigan upon Squall Lines and Summertime Convection - Walter A. Lyons

58. Angular Dependence of Reflection from Stratiform Clouds as Measured by TIROS IV Scanning Radiometers - A. Rabbe

59. Use of Wet-beam Doppler Winds in the Determination of the Vertical Velocity of Raindrops inside Hurricane Rainbands - T. Fujita, P. Black and A. Loesch

60. A Model of Typhoons Accompanied by Inner and Outer Rainbands - Tetsuya Fujita, Tatsuo Izawa., Kazuo Watanabe and Ichiro Imai

61. Three-Dimensional Growth Characteristics of an Orographic Thunderstorm System - Rodger A. Brown

62. Split of a Thunderstorm into Anticyclonic and Cyclonic Storms and their Motion as Determined from Numerical Model Experiments - Tetsuya Fujita and Hector Grandoso

63. Preliminary Investigation of Peripheral Subsidence Associated with Hurricane Outflow - Ronald M. Reap

64. The Time Change of Cloud Features in Hurricane Anna, 1961, from the Easterly Wave Stage to Hurricane Dissipation - James E. Arnold

65. Easterly Wave Activity over Africa and in the Atlantic with a Note on the Intertropical Convergence Zone during Early July 1961 - James E. Arnold

66. Mesoscale Motions in Oceanic Stratus as Revealed by Satellite Data - Walter A. Lyons and Tetsuya Fujita

67. Mesoscale Aspects of Orographic Influences on Flow and Precipitation Patterns - Tetsuya Fujita

68. A Mesometeorological Study of a Subtropical Mesocyclone -Hidetoshi Arakawa, Kazuo Watanabe, Kiyoshi Tsuchiya and Tetsuya Fujita

69. Estimation of Tornado Wind Speed from Characteristic Ground Marks - Tetsuya Fujita, Dorothy L. Bradbury and Peter G. Black

70. Computation of Height and Velocity of Clouds from Dual, Whole-Sky, Time-Lapse Picture Sequences - Dorothy L. Bradbury and Tetsuya Fujita

71. A Study of Mesoscale Cloud Motions Computed from ATS-I and Terrestrial Photographs - Tetsuya Fujita, Dorothy L. Bradbury, Clifford Murino and Louis Hull

72. Aerial Measurement of Radiation Temperatures over Mt. Fuji and Tokyo Areas and Their Application to the Determination of Ground- and Water-Surface Temperatures - Tetsuya Fujita, Gisela Baralt and Kiyoshi Tsuchiya

73. Angular Dependence of Reflected Solar Radiation from Sahara Measured by TIROS VII in a Torquing Maneuver - Rene Mendez.

74. The Control of Summertime Cumuli and Thunderstorms by Lake Michigan During Non-Lake Breeze Conditions - Walter A. Lyons and John W. Wilson

75. Heavy Snow in the Chicago Area as Revealed by Satellite Pictures - James Bunting and Donna Lamb

76. A Model of Typhoons with Outflow and Subsidence Layers - Tatsuo Izawa

* out of print

(continued on outside back cover)

MESOMETEOROLOGY PROJECT - - - RESEARCH PAPERS

(Continued from inside back cover)

77. Yaw Corrections for Accurate Gridding of Nimbus HRIR Data - Roland A. Madden

78. Formation and Structure of Equatorial Anticyclones Caused by Large-Scale Cross Equatorial Flows Determined by ATS-I Photographs - Tetsuya T. Fujita and Kazuo Watanabe and Tatsuo Izawa